



Doping powdered mining tailings with MgO and Al₂O₃ to fabricate cordierite ceramics

S. Kamara^{1,2,3*}

¹ Department of Chemical Engineering, School of Water and Environment, Chang'an University, Xi'an 710054, China; ksaidu2013@gmail.com(SK)

² Key Laboratory of Subsurface Hydrology and Ecology in Arid Areas, Ministry of Education, Chang'an University, Xi'an 710054, China

³ Department of Engineering, Faculty of Engineering and Technology, Ernest Bai Koroma University of Science and Technology, Magburaka, Sierra Leone

Received 01 Oct 2024,

Revised 30 Oct 2024,

Accepted 01 Nov 2024

Keywords:

- ✓ Experiment;
- ✓ Cordierite;
- ✓ Silica;
- ✓ Sintered;
- ✓ Characterization:

Citation: S. Kamara (2024) Doping powdered mining tailings with MgO and Al₂O₃ to fabricate cordierite ceramics, *J. Mater. Environ. Sci.*, 15(11), 1503-1515

Abstract: Cordierite is a magnesium and aluminum silicate compound with the chemical formula 2MgO.2Al₂O₃.5SiO₂. An experiment was done to synthesize ceramic materials using the mechanochemical method from six finely ground mine tailings. The objective was synthesizing cordierite ceramics from solid waste residues generated by mining and mineral processing activities. Each powdered specimen was doped with the appropriate stoichiometric amount of Al₂O₃ and MgO in jelly rubber cans and placed in a high-energy ball mill for 40 minutes to enhance the mixing and bond formation between the raw materials. The samples were sintered in a muffle furnace at 1100°C and 1200°C for 5 hours at a heating rate of 10°C per minute. This experimental procedure was repeated for all six mine tailings. All specimens were characterized using XRF, SEM, EDS, XRD, and FTIR techniques. Cordierite ceramics was synthesized in five of the six mine tailings alongside indalite and sapphirine which are aluminum and magnesium-rich silicate minerals. It was observed that cordierite crystals increase with an increase in temperature. The synthesis of cordierite alongside indalite and sapphirine from mine tailings is phenomenal and unprecedented and could be a significant novelty for materials scientists.

1. Introduction

Cordierite (2MgO.2Al₂O₃.5SiO₂) is a refractory material composed of magnesium oxide, alumina, and silica and it is hexagonal in structure (Albhillil, Kozánková, & Palou, 2014; Najim, 2021; Vakhula, Pona, Solokha, Koziy, & Petruk, 2021). It can be fabricated by using the sol-gel methods, solid-state reactions, crystallizing the glasses, mechanical milling, combustion process, and coprecipitation. The behavior of cordierite is better explained by the MgO-Al₂O₃-SiO₂ ternary system which contains several binary compounds like Enstatite (MgO.SiO₂) Mullite (3Al₂O₃.2SiO₂), Spinel (MgO.Al₂O₃) and Forsterite (2MgO.SiO₂) together with Cordierite and Sapphirine (4MgO.5Al₂O₃.2SiO₂) as a ternary system (El Buaishi, 2013; Yalamaç, 2004).

Among the various routes employed to fabricate cordierite, the solid-state reaction is prominently used in industry due to its simplicity and low production cost (Fotoohi, 2011; Hossain & Roy, 2020; Ogiwara, Noda, Shoji, & Kimura, 2010; Valášková, 2015). According to research, the first

stage formation of cordierite in the solid-state reaction begins at 1000°C between mullite, enstatite, and cristobalite and reaches a peak of 1275°C (Graf, 1961). In the second stage, the cordierite formed in the first stage now undergoes a fusion reaction with enstatite and cristobalite to form eutectic cordierite-enstatite silica liquid in the temperature range 1330°C to 1355°C. As the temperature increases, the liquid reacts with the remaining mullite, changing its composition to a typical mullite.

One of the most prominent phases of glass ceramics is cordierite which has a vast number of industrial applications due to its excellent mechanical properties, high refractoriness and durability, low thermal expansion, excellent thermal shock resistance, high chemical resistance, and low dielectric constant (de Brito et al., 2021; Elmaghraby, Ismail, & Belal, 2015; Kamara, Wang, & Ai, 2020; Khattab et al., 2021; Sembiring, Simanjuntak, Situmeang, Riyanto, & Sebayang, 2016; Zhang, et al., 2016) which are considered by material scientists consider for utilizing cordierite compounds to produce advanced composite materials. The production cost of cordierite from waste materials is less costly (Dong, Liu, Ma, & Meng, 2006; Tabit, Hajjou, Waqif, & Saâdi, 2021; Wang et al., 2019) and has electrical properties. Manufacturers of electronics, multilayer circuit boards, and thermal insulators utilize cordierite as substrate more than aluminum (Khater, El-Kheshen, & Farag, 2022). The applications of cordierite products in industries include refractories, heat insulation, filters, membranes, heating elements, microwaves, electromagnetic absorbers, etc (Gülzade Artun & AŞKIN, 2022; G Artun, Aşkın, & Tatar; Randhawa, 2023). Composite scientists utilize Mullite to increase the mechanical strength and thermal properties of cordierite. Cordierite-mullite composites are utilized in many applications like furnaces and catalytic support for the control of exhaust gas in automobiles (de Brito et al., 2021; Khattab, El-Rafei, & Zawrah, 2012; F. F. Li, Du, Zhang, Yang, & Shen, 2012; Marghussian, Balazadegan, & Eftekhari-Yekta, 2009). They also have excellent electrical insulating properties making them more useful in applications ranging from technical refractories to functional and structural ceramics.

Energy-saving cost is one of the most significant considerations in industries (Worrell, Blinde, Neelis, Blomen, & Masanet, 2010; Yoon et al., 2015). It is therefore essential to improve the thermal efficiency of industrial furnaces, particularly in ferrous and nonferrous industries. The cost of energy utilized in furnaces can be reduced effectively by using high-performance thermal insulating refractory materials for lining the inside of furnaces (M. Li et al., 2021; Salomão, Oliveira, Fernandes, Tiba, & Prado, 2022; Santos et al., 2017; Yurkov & Yurkov, 2017). This increases the use of insulating and low thermal conductivity materials. On the other hand, the new industrial demand requires the utilization of industrial waste materials as commercial products. The benefits of the new demands to transform industrial waste materials into useful commercial products are saving energy, saving natural resources, reducing the burden of waste disposal, and sinking the cost of refractory ceramic products (Cárcamo & Peñabaena-Niebles, 2022; Khanna et al., 2021). The use of these waste materials not only increases the performance but is also attractive to the environment, sustainability, and economy.

Over the years, industries are typically known for the consumption of materials, production of essential human needs, and generation of waste materials (Haas, Krausmann, Wiedenhofer, & Heinz, 2015; Hertwich, 2010). Waste recycling has some financial and ecological benefits. The growth of the Industrial Revolution has led to an increase in industrial waste that caused major social and environmental problems. Industrial wastes arising from human activities like mining, construction, and innovative technologies are now prominent environmental problems in many developing nations (Ferronato & Torretta, 2019; Hilson & Murck, 2000; Ngoc & Schnitzer, 2009; Omer, 2008; Song, Li, & Zeng, 2015). Some of the major environmental concerns are atmospheric contamination, storage space, and transportation. Transforming these wastes to produce useful industrial engineering materials

via green chemical methods will help to maintain a hygienic environment. Mining is well-known all over the world for the generation of solid waste residues from mineral processing which requires adequate management to maintain a clean and harmless environment (Ait-Khouia, Benzaazoua, & Demers, 2021; Bini, Maleci, & Wahsha, 2017; Edahbi, Plante, & Benzaazoua, 2019).

The purpose of this work is to synthesize cordierite ceramics from solid waste residues generated from mining and mineral processing that can be used in various refractory industrial applications. The characterization methods employed are XRF, SEM, EDS, XRD and FTIR technologies.

2. Materials and experimental processing procedures

2.1. Materials

The materials involved in this experimental research are aluminum oxide (Al_2O_3) and mine tailings obtained from different mining locations within the Shaanxi Province. The powdered mine tailings were characterized using XRF. **Table 1** below shows the measured amounts of the starting materials.

Table 1: Stoichiometric parameters of the raw materials for the synthesis of cordierite from mining tailings

	Wt of SiO_2 (g)	Wt of Al_2O_3 (g)	Wt of MgO (g)	Temperature ($^\circ\text{C}$)	
				1	2
Tailings 1	25	12	2	1100	1200
Tailings 2	25	14	4	1100	1200
Tailings 3	25	4	1.5	1100	1200
Tailings 4	25	12	4	1100	1200
Tailings 5	25	12	4	1100	1200
Tailings 6	25	16	6	1100	1200

2.2. Instruments

Analytical electronic balance, weighing papers, high energy grinding mill, thermostatic drier, muffle furnace (1300 $^\circ\text{C}$ maximum heating capacity), x-ray fluorescence (XRF), x-ray diffraction (XRD), scanning electron microscopy (SEM), energy dispersion x-ray spectroscopy (EDS), Fourier transform infrared (FTIR) and jade 6 and origin 9 software.

2.3. Processing and procedure

Figure 1 above illustrates the processing of six powdered samples of solid waste soil minerals (mining tailings) to synthesize cordierite refractories. The powdered tailings, alumina, and magnesium oxide shown in **Table 1** above were each measured using an electronic weighing scale as follows: sample one (25g of SiO_2 soil powder, 12g of Al_2O_3 and 2g of MgO), sample two (25g of SiO_2 soil powder, 14g of Al_2O_3 , and 4g of MgO), sample three (25g of SiO_2 soil powder, 4g of Al_2O_3 , and 1.5g MgO), sample four (25g of soil SiO_2 powder, 12g of Al_2O_3 , and 4g of MgO), sample five (25g of SiO_2 soil powder, 12g of Al_2O_3 , and 4g of MgO) and sample six (25 of SiO_2 soil powder, 16g of Al_2O_3 .and 6g of MgO). The measured samples were mixed separately using mortar and pestle, placed in a plastic holding container with some rubber balls, and then in a higher energy ball mill mixer for 40 minutes to enhance the reaction between the bonds in SiO_2 and Al_2O_3 . The samples for each soil mixture were partitioned into two and labeled according to their sintering temperatures as 1100 $^\circ\text{C}$ and 1200 $^\circ\text{C}$ and then taken to the muffle furnace sintering. In the muffle furnace, each sample was heated for 5 hours at 1100 $^\circ\text{C}$ and 1200 $^\circ\text{C}$ one at a time. The samples were sintered at a constant heating rate of 10 $^\circ\text{C}$ per

minute. The sintered specimens are removed from the furnace and prepared in powdered form for characterization. The sintered cordierite samples formed a hard mass of a substance that was very difficult to break after heating at 1200°C.

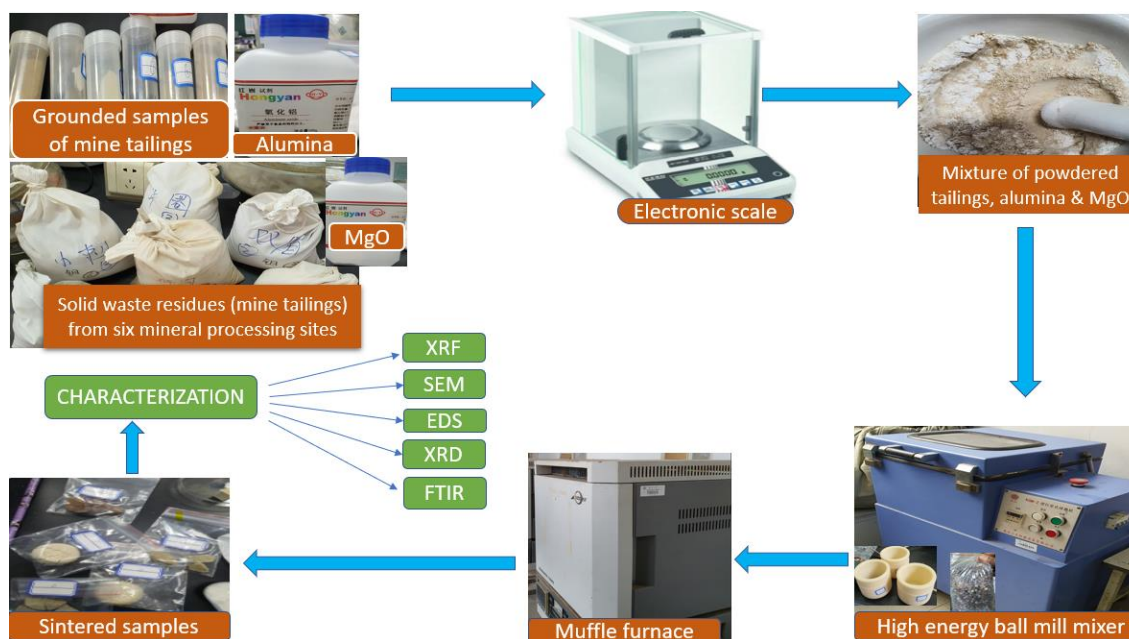


Figure 1: Experimental setup for the preparation of cordierite refractories from solid waste residue

3. Results and discussion

3.1. XRF analysis

Tables 2 & 3 below show the XRF analysis of the six mine tailings before and after sintering at 1100°C and 1200°C. This was done to determine if there were any significant changes in the composition and concentration of the chemical components in the samples. The XRF analysis was conducted on the cordierite samples to show the variation of chemical components present in the samples before and after sintering. It is observed that all six mine tailings have similar chemical components. The results shown in Tables 2, 3, & 4 indicate that there is a variation in concentrations of the chemical components in the samples before and after sintering. The concentrations vary significantly between the samples sintered at 1100°C and 1200°C.

The three compounds of interest in the samples that are essential for the fabrication of cordierite are SiO₂, Al₂O₃, and MgO. Analyzing the components shown in the two XRF tables, the dominant compound with the highest concentration is quartz (SiO₂) followed by alumina (Al₂O₃) and magnesia (MgO). The concentrations of quartz (SiO₂) were found to be in decrease in all samples sintered at 1200°C while the concentrations of alumina (Al₂O₃) and magnesia (MgO) increased considerably. This signifies that at higher temperatures the reaction between silica, alumina, and magnesia increased leading to the formation of the desired product. The other components, ranging from CaO to La₂O₃ in the samples, are impurities. CaO, Fe₂O₃, and K₂O have substantial concentrations which increase as the temperature of the samples increases while the other impurities are in minor concentrations. Chemical analysis of tailing samples provides valuable information about potential harmful trace elements such as heavy metals (Pb, Cu, Ni, Zn, etc.). The concentrations of the heavy metal oxides in the samples are insignificant and therefore do not pose any harm to the fabricated material.

Table 2: XRF data showing chemical compositions of mine tailings before sintering

	Tailing 1- w(M)/10 ⁻²	Tailing 2- w(M)/10 ⁻²	Tailing 3- w(M)/10 ⁻²	Tailing 4- w(M)/10 ⁻²	Tailing 5- w(M)/10 ⁻²	Tailing 6- w(M)/10 ⁻²
SiO ₂	68.8450	68.1548	80.9314	64.2001	65.4543	62.9568
Al ₂ O ₃	13.2346	12.5959	4.3694	13.0351	10.1224	14.0100
CaO	5.2342	6.4081	0.5437	6.1025	2.2971	8.3389
Fe ₂ O ₃	4.6198	4.7232	3.7008	6.1563	6.9628	4.3921
K ₂ O	4.3436	3.3055	1.8238	4,0843	4.1671	4.3625
MgO	1.3238	1.9691	0.4283	1.7251	1.7556	3.3856
Na ₂ O	0.9661	1.1063	0.0869	1.4858	0.3566	0.3993
TiO ₂	0.5188	0.5636	0.3600	0.6277	1.2130	0.4901
SO ₃	0.3493	0.5308	6.9270	1.1314	6.7737	0.9806
P ₂ O ₅	0.1803	0.2835	0.2273	0.2478	0.3218	0.1402
BaO	0.1393	0.0762	0.1432	0.5901	0.1738	0.1172
MnO	0.1102	0.1318	0.0422	0.1432	0.0723	0.2801
ZrO ₂	0.0329	0.0389	0.0608	0.0650	0.0004	0.0026
SrO	0.0328	0.0289	0.0693	0.1100	0.1134	0.0363
ZnO	0.0154	0.0116	0.0092	0.1709	0.0138	0.0181
PbO	0.0146	0.0288	0.0452	0.0136
Cr ₂ O ₃	0.0136	0.0155	0.0193	0.0209	0.0127	0.0245
CuO	0.0132	0.0112	0.0193	0.0115	0.0141	0.0467
Rb ₂ O	0.0126	0.0102	0.0071	0.0112	0.0192	0.0115
NiO	0.0061	0.0071	0.0069	0.0068
MoO ₃	0.0433	0.0192
NbO
Y ₂ O ₃
Ra
CeO ₂	0.1497	0.0362
La ₂ O ₃	0.0386
WO ₃	0.0289
In ₂ O ₃	0.0261
TOTAL	100.0001	100.0000	100.0002	99.999	99.999	99.999

Table 3: XRF concentrations of chemical components in the cordierite samples sintered at 1100°C

	Tailing 1- w(M)/10 ⁻²	Tailing 2- w(M)/10 ⁻²	Tailing 3- w(M)/10 ⁻²	Tailing 4- w(M)/10 ⁻²	Tailing 5- w(M)/10 ⁻²	Tailing 7- w(M)/10 ⁻²
SiO ₂	67.6838	67.7249	80.7885	64.3718	65.1172	62.1140
Al ₂ O ₃	13.6710	12.8391	4.7125	13.1646	10.1860	14.2713
MgO	1.8098	2.0081	0.4771	1.7139	1.8252	3.5330
CaO	5.3701	6.4393	0.5826	6.0534	2.3057	8.4528
Fe ₂ O ₃	4.7045	4.8723	3.7713	6.1493	7.1253	4.5071
K ₂ O	4.2709	4.8723	1.9777	4.1013	4.1359	4.4204
Na ₂ O	0.9868	3.3192	0.0926	1.4164	0.3568	0.4226
TiO ₂	0.5274	1.0773	0.3954	0.6101	1.2292	0.5130
P ₂ O ₅	0.1737	0.5739	0.2360	0.2533	0.3269	0.1353
BaO	0.1465	0.2746	0.1660	0.5562	0.1896	0.1065
MnO	0.1144	0.0673	0.0465	0.1477	0.0741	0.2934
SrO	0.0329	0.1306	0.0761	0.1086	0.1148	0.0370

ZrO ₂	0.0387	0.0286	0.0412	0.0544	0.0053	0.0036
PbO	0.0154	0.0386	0.0446	0.0131
ZnO	0.0140	0.0299	0.0112	0.1668	0.0132	0.0178
CuO	0.0125	0.0114	0.0205	0.0121	0.0132	0.0489
Rb ₂ O	0.0136	0.0118	0.0069	0.0115	0.0191	0.0125
SO ₃	0.3552	0.0109	6.4180	1.0071	6.8490	1.0745
NiO	0.0051	0.5199	0.0065	0.0079
In ₂ O ₃	0.0266	0.0058
MnO ₃	0.0612	0.0829
Cr ₂ O ₃	0.0272	0.0115	0.0191	0.0177	0.0283
Y ₂ O ₃	0.0165
Br
WO ₃	0.0314
NbO
Ra
CeO ₂	0.0571
La ₂ O ₃	0.0502
TOTAL	100.0001	100.0000	100.0001	100.0001	100.0002	99.9999

Table 4: XRF concentrations of chemical components in the cordierite samples sintered at 1200°C

	Tailing 1- w(M)/10 ⁻²	Tailing 2- w(M)/10 ⁻²	Tailing 3- w(M)/10 ⁻²	Tailing 4- w(M)/10 ⁻²	Tailing 5- w(M)/10 ⁻²	Tailing 6- w(M)/10 ⁻²
SiO ₂	42.5898	37.8483	54.3840	37.7768	41.2178	32.4220
Al ₂ O ₃	34.6513	36.4057	23.5207	33.8209	32.3989	35.8652
MgO	14.6808	19.1239	18.1884	19.9269	20.6985	25.1113
CaO	2.4414	2.3217	0.3564	2.6439	0.7512	2.9348
Fe ₂ O ₃	2.2564	2.0642	2.0610	2.4157	2.5174	1.5800
K ₂ O	2.0841	1.1934	0.7995	1.5485	1.4225	1.1726
Na ₂ O	0.7321	0.5551	0.1428	0.6856	0.2019	0.1521
TiO ₂	0.2496	0.2297	0.1561	0.2942	0.4452	0.1760
P ₂ O ₅	0.1224	0.1186	0.0754	0.1333	0.1015	0.0712
BaO	0.0764	0.0668	0.4029	0.0739
MnO	0.0568	0.0586	0.0141	0.0572	0.0268	0.1074
SrO	0.0162	0.0102	0.0214	0.0546	0.0422	0.0112
ZrO ₂	0.0136	0.0098	0.0163	0.0056	0.0051	0.0013
PbO	0.0085	0.0114	0.1088
ZnO	0.0081	0.0056	0.0038	0.0047	0.0069	0.0073
CuO	0.0070	0.0032	0.0085	0.0042	0.0060	0.0206
Rb ₂ O	0.0055	0.0279	0.0466	0.0556	0.0029
SO ₃	0.0038	0.1654	0.0037	0.3506
NiO	0.0181	0.0042
In ₂ O ₃	0.0238
MnO ₃	0.0195	0.0119
Cr ₂ O ₃	0.0094
Y ₂ O ₃
Br	0.0214
WO ₃
NbO
Ra
CeO ₂
La ₂ O ₃
TOTAL	100.0000	100.0000	100.0001	99.9999	100.0003	100.0001

On the other hand, the oxides of Si and Al reported in the XRF results shown in Tables 2, 3, & 4 are mostly illite and quartz. The oxide of Fe has a higher percentage, indicating that the smectite has a rich iron content. Rutile mineral was also discovered by the presence of Ti oxide but in a lower concentration. P_2O_5 characterizes the presence of apatite minerals but it is sometimes considered to originate from phosphate fertilizer in cases where the apatite mineral is not indicated from the XRD analysis.

3.2. SEM Analysis

One of the most widely used techniques to identify and characterize mineral samples and ceramic materials is the SEM. Figure 2 represents the SEM micrographs of six sintered samples prepared for the fabrication of cordierite ceramics. A cubic and bulky mass of the crystalline materials is observed in samples 1 to 4 while the 5th and 6th samples have their materials separated from each other with the sixth being highly porous. There is a decrease in the strength of the materials whose crystalline materials do not interlock with each other.

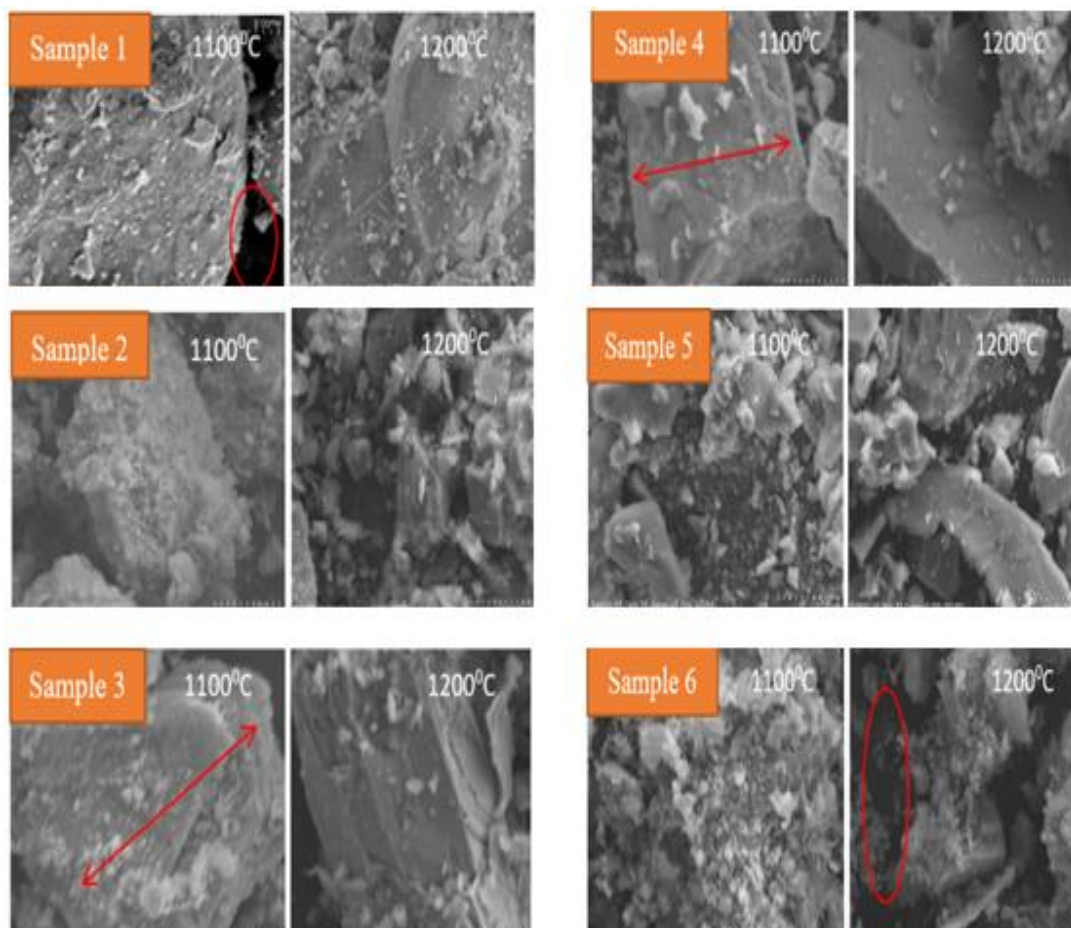


Figure 2: SEM micrographs of samples sintered at 1100°C and 1200°C

On the contrary, smaller octahedral crystals have a higher contact area and thus can better distribute the stress within the material. It has been reported that the mechanical strength of composite materials depends on the size, concentration, and matrix interface of the particles. The SEM morphological analysis was carried out on the samples to allow the identification of the crystalline materials. A semi-quantitative analysis of elements also performed on the samples using SEM-EDS displays the same

characteristics as those discussed above. The result of the micrographs shows hexagonal platelets of the specimens in non-uniform size.

3.3. EDS Analysis

The above EDS tables and micrographs are representations from each of the six samples prepared for the fabrication of cordierite refractory ceramics. They show the percentage weights of elements in the compounds of the various in the various samples. The identified elements and their corresponding compounds according to the EDS results are O from SiO₂, Mg from MgO, Al from Al₂O₃, and Si from SiO₂ except for sample five where Al and its corresponding Al₂O₃ compound were not identified. The EDS was purposely carried out to determine the components present in the samples that are suitably required for the synthesis of cordierite refractory materials at high temperatures. The three main required compounds for the formation of cordierite are silica (SiO₂), alumina (Al₂O₃), and magnesia (MgO). Referencing the XRF results in section 3.1 above, there are numerous other components present in the samples under investigation in smaller quantities but were not present in the EDS characterization data shown in figure 3 above. This is simply because the EDS does not identify sample components that are not in significant quantities. It is observed that the percentage weights of elements across the six samples are in significant amounts except in sample 5 where the percentage weight of Al was not recorded. The EDS data is consistent with the XRD data in Figure 4 below where the evolution of cordierite was not observed in the 5th and 6th samples. The EDS micrographs show that all the six samples were scanned at 20 um.

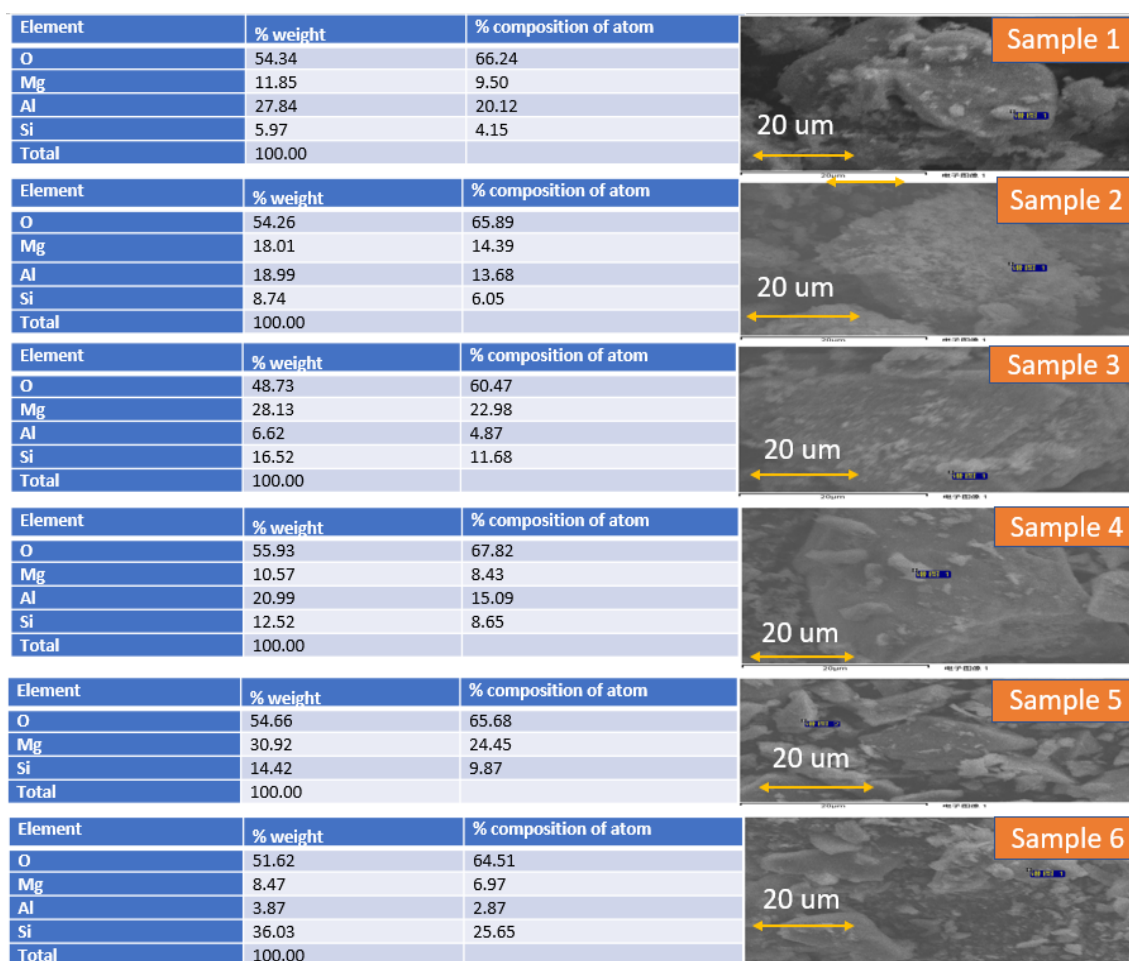


Figure 3: EDS data and micrographs of samples prepared for the fabrication of cordierite ceramics

3.4. XRD analysis

Figure 4 above depicts the XRD spectrum of six samples processed for the fabrication of cordierite refractory ceramics. Each of the six samples was sintered at 1100°C and 1200°C. The XRD data obtained was analyzed using jade and origin software. According to the analysis, cordierite (PDF# = 13-0294), indalite (PDF# = 48-1600), and sapphirine (PDF# = 21-1152) were the major crystalline phases discovered in the samples. At 1100°C, the cordierite was formed at the angles $2\theta=26.6^\circ$ and 37.0° at intensities (I)=436 and 34. The 2θ angles at which cordierite crystallizes at 1200°C are 18.2° , 21.5° , 26.3° , 28.3° , 29.2° , 33.7° , and 36.7° at intensities (I) of 111, 188, 186, 205, 83, 74 and 78 respectively. A higher number of cordierite crystals were observed in samples sintered at 1200°C compared to those synthesized at 1100°C. This signifies that the formation of cordierite refractories increases with an in temperature.

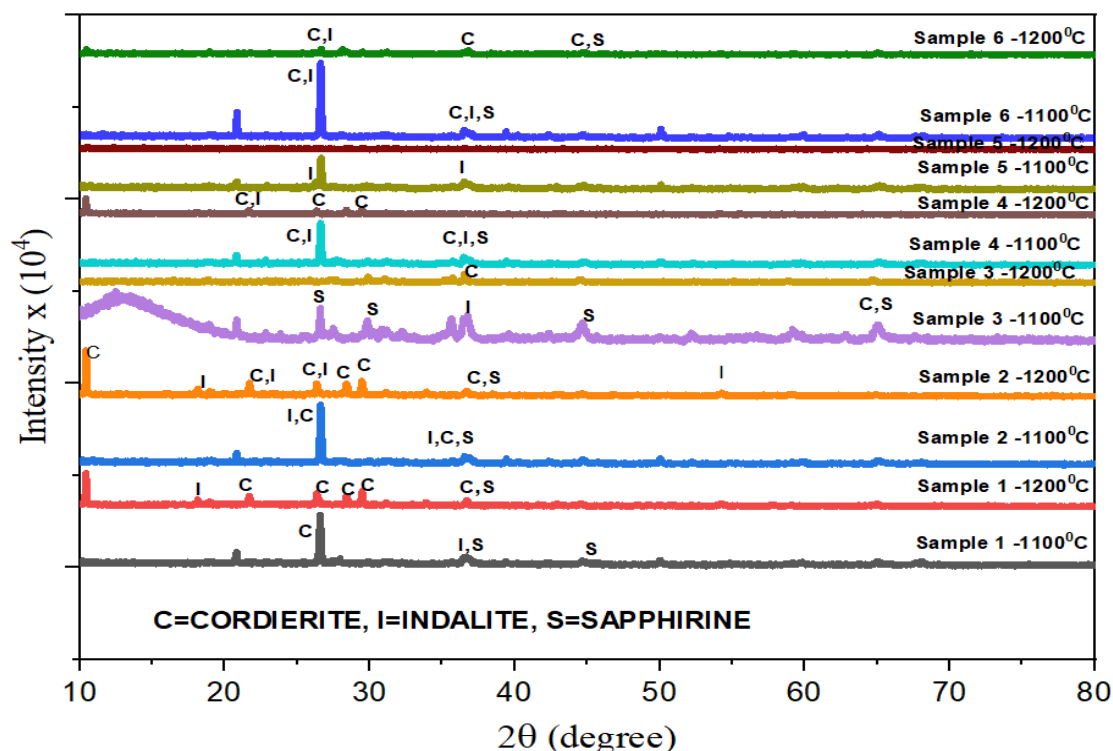


Figure 4: XRD spectrum of samples showing the evolution of cordierite ceramics sintered at 1100°C and 1200°C

The pattern of evolution of cordierite refractories shown in Figure 4 both at 1100°C and 1200°C in sample two is the same as those in one. The evolution of cordierite crystals at a sintering temperature of 1100°C was observed at the angles $2\theta=26.3^\circ$ and 36.6° at intensities of 333 and 53. The third sample according to the XRD spectrum above appears to be more amorphous both at 1100°C and 1200°C with the evolution of single crystalline cordierite phases at 44.7° and 36.3° respectively. Sapphirine crystals are more pronounced in Sample 3. Interestingly, only one crystalline material is synthesized at 1200 °C. Samples 3, 4, 5, and 6 exhibit a pattern where all crystals at 1200 °C are formed at very low intensities, except for Sample 5, which shows no crystalline ceramic material, as indicated by the XRD figure above. This suggests that Sample 5 is completely amorphous. In samples four and six, the angle at which the cordierite phase was formed at 1100°C is 36.7° at intensities of 26 and 43 while at 1200°C, the angles and intensities at which cordierite refractory crystallizes are $2\theta=26.2^\circ$, 36.5° , 21.7° , 28.4° , 29.4° and I=86, 43, 93, 104 & 123 respectively. According to the XRD analysis, cordierite refractory ceramic was not synthesized at either sintering temperature in sample 5. This could be due to inappropriate stoichiometric mixtures of the initial materials or inadequate mixing in the

high-energy ball mill, preventing proper reaction and bond formation. Another reason could be insufficient sintering of the sample. Generally, the evolution of cordierite ceramic increases with temperature across all samples, except for sample 5, where cordierite was not synthesized. The presence of indialite and sapphirine alongside cordierite was unexpected.

3.5. FTIR analysis

The FTIR spectrum in [Figure 5](#) above shows the results of samples prepared from six different mining tailings, five of which successfully show the evolution of cordierite ceramics sintered at 1100°C and 1200°C, according to the XRD analysis in [section 3.4](#). The sharp peak at 1588cm⁻¹ corresponds to the Si-O-Si stretching vibration of quartz, observed in all samples heated at 1100 °C and 1200 °C. The downward peak in the sixth sample heated at 1200 °C results from low energy transmittance, indicating molecular vibrations at specific frequencies.

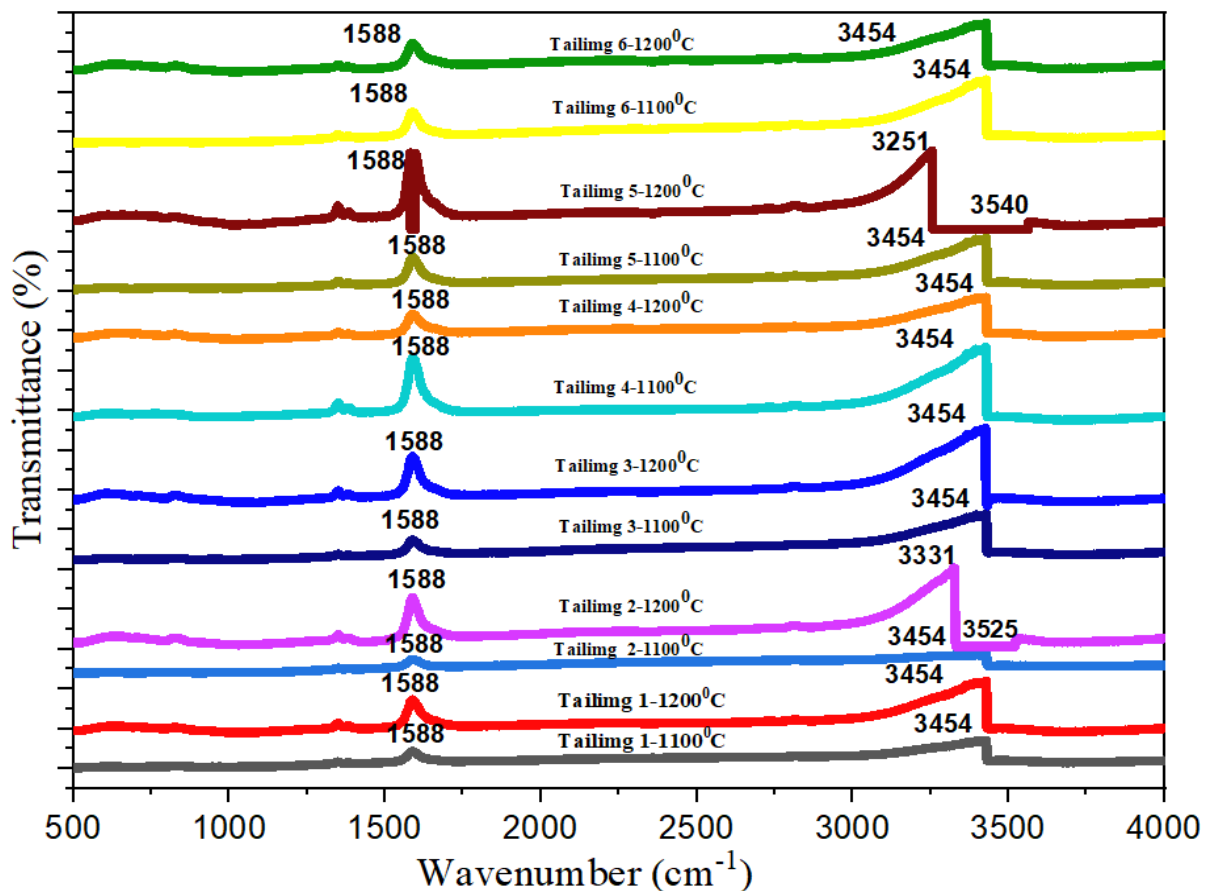


Figure 5: FTIR spectra showing the absorption bands of samples sintered at 1100°C and 1200°C

The absorption bands at 3454cm⁻¹, 3525cm⁻¹, 333cm⁻¹, and 3251cm⁻¹ correspond to the bending vibrations of the Al-O-Al functional group in the alumina compound. According to the FTIR spectral result of the tailing samples, the wavenumber 3454cm⁻¹ is observed in tailings 1, 3, 4, and 6 with varying percentage transmittance. There is an increase in transmittance for tailings 1, 3, and 4 when the temperature is raised from 1100°C to 1200°C while tailing 6 shows a slight decrease in transmittance with the temperature increase. Tailings 2 and 5 exhibit variations in wavenumbers when their temperatures are increased from 1100°C to 1200°C. Tailing 2 shows a wavenumber of 3454cm⁻¹ at 1100°C, and 3331cm⁻¹, and 3525cm⁻¹ at 1200°C. Similarly, tailing 5 has the same wavenumber as tailing 2 at 1100°C but differs at 1200°C.

4 Summary

Powdered forms of six mining tailings from different locations were each mixed with silica and magnesia. These mixtures were placed in a high-energy ball mill and sintered in a muffle furnace at 1100 °C and 1200 °C. The specimens were characterized using XRF, SEM, EDS, XRD, and FTIR techniques, which determined the chemical compositions, morphology, crystallinity, and absorption bands of the materials. XRD analysis revealed the formation of cordierite ceramics in five out of the six samples, along with indalite and sapphirine minerals. The simultaneous discovery of cordierite, indalite, and sapphirine in this experiment is unprecedented, remarkable, and a significant novelty of this research.

Acknowledgments: This work was supported by the National Natural Science Foundation of China. Thanks to Wang Wei (School of Water Resources and Environment, Chang'an University) for the adequate supervision and providing the platform to carry out this research successfully.

Conflicts of Interest: The authors declare no conflict of interest.

References

- Ait-Khouia, Y., Benzaazoua, M., & Demers, I. (2021). Environmental desulfurization of mine wastes using various mineral processing techniques: Recent advances and opportunities. *Minerals Engineering*, 174, 107225. <http://dx.doi.org/10.1016/j.mineng.2021.107225>
- Albhillil, A. A., Kozánková, J., & Palou, M. (2014). Thermal and microstructure stability of cordierite–mullite ceramics prepared from natural raw materials. *Arabian Journal for Science and Engineering*, 39, 67-73. <http://dx.doi.org/10.1007/s13369-013-0863-z>
- Artun, G., & Aşkin, A. (2022). Studies on Production of Low-Cost Ceramic Membranes and Their Uses in Wastewater Treatment Processes. *The European Journal of Research and Development*, 2(2), 126-140. <http://doi.org/10.56038/ejrnd.v2i2.39>
- Artun, G., Aşkin, A., & Tatar, İ. (2023) Production of Cordierite Based Ceramic Membrane from Magnesite Waste, *Conference: WCCE11 11th World Congress of Chemical Engineering*.
- Bini, C., Maleci, L., & Wahsha, M. (2017). Mine waste: assessment of environmental contamination and restoration *Assessment, restoration and reclamation of mining influenced soils* (pp. 89-134): Elsevier. <http://dx.doi.org/10.1016/B978-0-12-809588-1.00004-9>
- Cárcamo, E. A. B., & Peñabaena-Niebles, R. (2022). Opportunities and challenges for the waste management in emerging and frontier countries through industrial symbiosis. *Journal of Cleaner Production*, 363, 132607. <http://dx.doi.org/10.1016/j.jclepro.2022.132607>
- de Brito, I. P., de Almeida, E. P., de Araújo Neves, G., et al. (2021). Development of cordierite/mullite composites using industrial wastes. *International Journal of Applied Ceramic Technology*, 18(1), 253-261. <http://dx.doi.org/10.1111/ijac.13622>
- Dong, Y., Liu, X., Ma, Q., & Meng, G. (2006). Preparation of cordierite-based porous ceramic micro-filtration membranes using waste fly ash as the main raw materials. *Journal of membrane science*, 285(1-2), 173-181. <http://dx.doi.org/10.1016/j.memsci.2006.08.032>
- Edahbi, M., Plante, B., & Benzaazoua, M. (2019). Environmental challenges and identification of the knowledge gaps associated with REE mine wastes management. *Journal of Cleaner Production*, 212, 1232-1241. <http://dx.doi.org/10.1016/j.jclepro.2018.11.228>
- El Buaishi, N. M. (2013). Sinterability of cordierite powders synthesized by different sol-gel methods. *Универзитет у Београду*.
- Elmaghraby, M., Ismail, A., & Belal, Z. (2015). Thermal expansion, physico-mechanical properties and microstructure of cordierite synthesized from different starting materials. *Interceram-International Ceramic Review*, 64, 209-213. <http://dx.doi.org/10.1007/bf03401125>

- Ferronato, N., & Torretta, V. (2019). Waste mismanagement in developing countries: A review of global issues. *International journal of environmental research and public health*, 16(6), 1060. <http://dx.doi.org/10.3390/ijerph16061060>
- Fotoohi, B. (2011). *A study of mechanochemical activation in solid-state synthesis of advanced ceramic composites*. University of Birmingham, UK.
- Graf, R. B. (1961). *Reactions in the System Magnesium-Oxide-Aluminum-Oxide-Silicon-Dioxide as Examined by Continuous High-Temperature X-Ray Diffraction*: University of Illinois at Urbana-Champaign. <http://hdl.handle.net/2142/56744>
- Haas, W., Krausmann, F., Wiedenhofer, D., & Heinz, M. (2015). How circular is the global economy?: An assessment of material flows, waste production, and recycling in the European Union and the world in 2005. *Journal of industrial ecology*, 19(5), 765-777. <http://dx.doi.org/10.1111/jiec.12244>
- Hertwich, E. (2010). *Assessing the environmental impacts of consumption and production: priority products and materials*: UNEP/Earthprint.
- Hilson G., Murck B. (2000). Sustainable development in the mining industry: clarifying the corporate perspective. *Resources Policy*, 26(4), 227-238. [http://dx.doi.org/10.1016/S0301-4207\(00\)00041-6](http://dx.doi.org/10.1016/S0301-4207(00)00041-6)
- Hossain, S. S., & Roy, P. (2020). Sustainable ceramics derived from solid wastes: A review. *Journal of Asian Ceramic Societies*, 8(4), 984-1009. <http://dx.doi.org/10.1080/21870764.2020.1815348>
- Kamara, S., Wang, W., & Ai, C. (2020). Fabrication of Refractory Materials from Coal Fly Ash, Commercially Purified Kaolin, and Alumina Powders. *Materials*, 13(15), 3406. <http://dx.doi.org/10.3390/ma13153406>
- Khanna R., Konyukhov Y., Burmistrov I., Cayumil R., Belov V., ... Mukherjee, P. (2021). An innovative route for valorising iron and aluminium oxide rich industrial wastes: Recovery of multiple metals. *Journal of Environmental Management*, 295, 113035. <https://doi.org/10.1016/j.jenvman.2021.113035>
- Khater, G. A., El-Kheshen, A. A., & Farag, M. M. (2022). Synthesis and Characterization of Cordierite and Wollastonite Glass—Ceramics Derived from Industrial Wastes and Natural Raw Materials. *Materials*, 15(10), 3534. <http://dx.doi.org/10.3390/ma15103534>
- Khattab, R., Abo-Elmagd, H., Ajiba, N., et al. (2021). Sintering, physicochemical, thermal expansion and microstructure properties of cordierite ceramics based on utilizing silica fume waste. *Materials Chemistry and Physics*, 270, 124829. <http://dx.doi.org/10.1016/j.matchemphys.2021.124829>
- Khattab, R., El-Rafei, A., & Zawrah, M. (2012). In situ formation of sintered cordierite–mullite nano–micro composites by utilizing of waste silica fume. *Materials Research Bulletin*, 47(9), 2662-2667. <http://dx.doi.org/10.1016/j.materresbull.2012.04.036>
- Li, F. F., Du, J., Zhang, M. X., Yang, W. C., & Shen, Y. (2012). Preparation of cordierite–mullite composite crucibles and structure characterization. *Advanced Materials Research*, 430, 521-524. <https://doi.org/10.4028/www.scientific.net%2FAMR.430-432.521>
- Li, M., Zheng, F., Xiao, Y., Guan, Y., Wang, J., Zhen, Q., & Yu, Y. (2021). Utilization of residual heat to prepare high performance foamed glass-ceramic from blast furnace slag and its reinforce mechanism. *Process Safety and Environmental Protection*, 156, 391-404.
- Marghussian, V., Balazadegan, O., & Eftekhari-Yekta, B. (2009). Crystallization behaviour, microstructure and mechanical properties of cordierite–mullite glass ceramics. *Journal of Alloys and Compounds*, 484(1-2), 902-906. <http://dx.doi.org/10.1016/j.jallcom.2009.05.080>
- Najim, M. M. (2021). Synthesis of industrial ceramic (cordierite) from Iraqi raw materials through solid-state sintering method. *The Iraqi Geological Journal*, 23-34. <https://doi.org/10.46717/igj.54.1A.3Ms-2021-01-24>
- Ngoc U.N., Schnitzer H. (2009). Sustainable solutions for solid waste management in Southeast Asian countries. *Waste management*, 29(6), 1982-1995. <http://dx.doi.org/10.1016/j.wasman.2008.08.031>

- Ogiwara, T., Noda, Y., Shoji, K., & Kimura, O. (2010). Solid state synthesis and its characterization of high density cordierite ceramics using fine oxide powders. *Journal of the Ceramic Society of Japan*, 118(1375), 246-249. <http://dx.doi.org/10.2109/jcersj2.118.246>
- Omer, A. M. (2008). Energy, environment and sustainable development. *Renewable and Sustainable Energy Reviews*, 12(9), 2265-2300. <http://dx.doi.org/10.1016/j.rser.2007.05.001>
- Randhawa, K. S. (2023). A state-of-the-art review on advanced ceramic materials: fabrication, characteristics, applications, and wettability. *Pigment & Resin Technology*. <https://doi.org/10.1108/PRT-12-2022-0144>
- Salomão, R., Oliveira, K., Fernandes, L., Tiba, P., & Prado, U. (2022). Porous Refractory Ceramics for High-Temperature Thermal Insulation-Part 2: The Technology Behind Energy Saving. *Interceram-International Ceramic Review*, 71(1), 38-50.
- Santos, M., Moreira, M., Campos, M., Pelissari, P., Angelico, R., Sako, E., . . . Refractories, P. (2017). Steel ladle energy saving by refractory lining desing. *insulating materials*, 3(4), 5-6.
- Sembiring, S., Simanjuntak, W., Situmeang, R., Riyanto, A., & Sebayang, K. (2016). Preparation of refractory cordierite using amorphous rice husk silica for thermal insulation purposes. *Ceramics International*, 42(7), 8431-8437. <http://dx.doi.org/10.1016/j.ceramint.2016.02.062>
- Song, Q., Li, J., & Zeng, X. (2015). Minimizing the increasing solid waste through zero waste strategy. *Journal of Cleaner Production*, 104, 199-210. <http://dx.doi.org/10.1016/j.jclepro.2014.08.027>
- Tabit, K., Hajjou, H., Waqif, M., Saâdi, L. (2021). Cordierite-based ceramics from coal fly ash for thermal and electrical insulations. *Silicon*, 13, 327-334. <https://link.springer.com/article/10.1007/s12633-020-00428-y>
- Vakhula, O., Pona, M., Solokha, I., Koziy, O., Petruk, M. (2021). Ceramic protective coatings for cordierite-mullite refractory materials. *Chemistry and Chemical Technology*, 15(2), 247-253. <http://dx.doi.org/10.23939/chcht15.02.247>
- Valášková M. (2015). Clays, clay minerals and cordierite ceramics-A review, *Ceramics - Silikáty* 59(4), 331-340
- Wang, S., Wang, H., Chen, Z., Ji, R., Liu, L., & Wang, X. (2019). Fabrication and characterization of porous cordierite ceramics prepared from fly ash and natural minerals. *Ceramics International*, 45(15), 18306-18314.
- Worrell, E., Blinde, P., Neelis, M., Blomen, E., & Masanet, E. (2010). Energy efficiency improvement and cost saving opportunities for the US iron and steel industry an ENERGY STAR (R) guide for energy and plant managers: Lawrence Berkeley National Lab.(LBNL), Berkeley, CA (United States).
- Yalamaç, E. (2004). *Preparation of fine spinel and cordierite ceramic powders by mechano-chemical techniques*: Master of Science, Izmir Institute of Technology (Turkey). <http://dx.doi.org/10.13140/RG.2.1.1627.7527>
- Yoon, H.-S., Kim, E.-S., Kim, M.-S., Lee, J.-Y., Lee, G.-B., & Ahn, S.-H. (2015). Towards greener machine tools—A review on energy saving strategies and technologies. *Renewable and Sustainable Energy Reviews*, 48, 870-891.
- Yurkov, A., & Yurkov, A. (2017). Refractories and Heat Insulation Materials for Cast Houses. *Refractories for Aluminum: Electrolysis and the Cast House*, 229-266. http://dx.doi.org/10.1007/978-3-319-53589-0_3
- Zhang, L., Olhero, S., & Ferreira, J. M. (2016). Thermo-mechanical and high-temperature dielectric properties of cordierite-mullite-alumina ceramics. *Ceramics International*, 42(15), 16897-16905. <http://dx.doi.org/10.1016/j.ceramint.2016.07.188>
- (2024) ; <http://www.jmaterenvirosci.com>